PCCP

The many-body expansion for aqueous systems revisited: III. Hofmeister ion – water interactions

Journal:	*Physical Chemistry Chemical Physics*
Manuscript ID	CP-ART-01-2021-000409.R2
Article Type:	Paper
Date Submitted by the Author:	30-Mar-2021
Complete List of Authors:	Herman, Kristina; University of Washington, Chemistry Heindel, Joseph; University of Washington, Chemistry Xantheas, Sotiris; Pacific Northwest National Laboratory, Physical Sciences Division

The many-body expansion for aqueous systems revisited: III. Hofmeister ion – water interactions

Kristina M. Herman,[a] Joseph P. Heindel[a] and Sotiris S. Xantheas[a, b, *]

[a] Department of Chemistry, University of Washington, Seattle, WA 98195, USA

[b] Advanced Computing, Mathematics and Data Division, Pacific Northwest National Laboratory, 902 Battelle Boulevard, P.O. Box 999, MS K1-83, WA, 99352, USA

Abstract

We report a Many Body Energy (MBE) analysis of aqueous ionic clusters containing anions and cations at the two opposite ends of the Hofmeister series, viz. the kosmotropes Ca^{2+}, SO_4^{2-} and chaotropes NH_4^+ and ClO_4^- with 9 water molecules to quantify the how these ions in altering the interaction between the water molecules in their immediate surrounding. We specifically aim at quantifying how various ions (depending on their position in the Hofmeister series) affect the interaction between surrounding water molecules and probe whether there is a qualitatively different behavior between the kosmotropic vs. chaotropic ions. The current results when compared to the ones reported earlier for water clusters [J. P. Heindel and S. S. Xantheas, *J. Chem. Theor. Comput.* **16** (11), 6843–6855 (2020)] as well as for alkali metal and halide ion aqueous clusters of the same size [J. P. Heindel and S. S. Xantheas, *J. Chem. Theor. Comput.* in press (2020); https://dx.doi.org/10.1021/acs.jctc.0c01309], which lie in the middle of the Hofmeister series, offer a complete account of the effect of an ion across the Hofmeister series from "kosmotropes" to "chaotropes" has on the interaction between neighboring water molecules. Through this analysis, noteworthy differences between the MBE of kosmotropes and chaotropes were identified. The MBE of kosmotropes is dominated by ion-water interactions that extend

* Corresponding author. Email: sotiris.xantheas@pnnl.gov and xantheas@uw.edu

beyond the 4-body term, the rank at which the MBE of pure water converges. The percentage contribution of the 2-B to the total cluster binding energy is noticeably larger. The disruption of the hydrogen bonded network due to the dominant ion-water interactions result in weak, unfavorable water-water interactions. The MBE for chaotropes, on the other hand, was found to converge more quickly as it more closely resembles that of pure water clusters. Chaotropes exhibit weaker overall binding energies and weaker ion-water interactions in favor of water-water interactions, somewhat recovering the pattern of the 2-4 body terms exemplified by pure water clusters. A remarkable anti-correlation between the 2-B ion-water (I-W) and water-water (W-W) interactions as well as between the 3-B (I-W-W) and (I-W) interactions was found for both kosmotropic and chaotropic ions. This anti-correlation is linear for both the monatomic anions and the monatiomic cations, suggesting the existence of underlying physics that were previously unexplored. The consideration of two different structural arrangements (ion inside and outside of a water cluster) suggests that fully solvated (ion inside) chaotropes disrupt the hydrogen bonding network in a similar manner as partially solvated (ion outside) kosmotropes and offer useful insights into the modeling requirements of bulk vs. interfacial ion solvation. It is noteworthy that the 2-B contribution to the total Basis Set Superposition Error (BSSE) correction for both the kosmotropic and chaotropic ions follows the universal erf profile vs. intermolecular distance previously reported for pure water, halide ion-water and alkali metal ion-water clusters. When scaled for the corresponding dimer energies and distances, a single profile fits the current results together with all previously reported ones for the pure water and halide water clusters. This finding lends further support to schemes for accurately estimating the 2-B BSSE correction in condensed environments.

I. Introduction

The Hofmeister series was originally established in the 1880s by Franz Hofmeister to order cations and anions based on their efficacy in precipitating proteins from an aqueous solution containing egg-white.[1,2] This same ordering was later found to be related to protein and hydrocarbon stability in solution as well as other properties that do not involve proteins, like surface tension and viscosity.[3–6] While some research has examined the interplay of ions with the protein backbone and amino acid residues to explain the salting-out properties of ions,[7–22] recent physical chemistry research[23–43] has been focused on understanding the dynamical and structural impacts that specific ions may have on liquid water and the physical mechanism underlying these effects.

The Hofmeister series orders cations and anions, respectively, in the following manner:

$$\mathrm{CO_3^{2-} > SO_4^{2-} > H_2PO_4^- > F^- > Cl^- > Br^- > NO_3^- > I^- > ClO_4^- > SCN^-}$$

$$\mathrm{Ca^{2+} > Li^+ > Na^+ > K^+ > Cs^+ > NH_4^+ > N(CH_3)_4^+} \quad (1)$$

The ions at opposing ends of the Hofmeister series are termed kosmotropes (left) and chaotropes (right), or "structure-makers" and "disorder-makers"/"structure-breakers", respectively. Kosmotropes efficiently salt proteins out of solution, stabilize the 3-dimensional configuration of proteins, and increase the surface tension and viscosity of solutions, while chaotropes behave in the opposite manner. Although the terms, "structure-makers" and "disorder-makers", seem to imply the ion's effect on water molecules, the role ions play in water and the extent to which they can influence distant solvation shells is highly contested. Perhaps the most widely debated component of this research is determining what it means for an ion to be structure-making, how it manifests itself, and how this ability can be measured or observed. This ambiguity has led to many different interpretations and hypotheses regarding the Hofmeister effect.

Several different metrics have been used to gain insight into the Hofmeister effect; some focusing on the range of the ion's influence on the surrounding water molecules and others on the structural changes in the hydrogen bonding network as a result of the ion. Thermodynamic studies on the entropy and Gibbs energy of solvation[27] and terahertz echo experiments[24] have both suggested that Hofmeister ions cause structural changes in the hydrogen bonding network which result in different entropic quantities (as a measure of order) and decay times within the water-

water modes of aqueous systems. The presence of the "dangling O-H" in aqueous nanodroplets,[28–30] red- and blue-shifting of the bending mode of water,[31] deviations in neutron diffraction reminiscent of water's behavior at high pressures,[32,44] and orientational order measured by femtosecond elastic second harmonic scattering experiments[23] have supported a relatively long-range influence of kosmotropes, extending to or exceeding three solvation shells. However, the hindrance of water rotations in solely the innermost solvation shell using femtosecond pump-probe spectroscopy[33], the negligible changes in relaxation time of the bulk hydrogen bond network of various anionic Hofmeister systems from dielectric relaxation spectroscopy experiments,[34] and diminished hydrogen bonding of water molecules only in the first solvation shell relative to bulk water[35] suggested water-water interactions are not actually disrupted or influenced beyond the first solvation shell. X-ray emission spectroscopy found contradicting results, finding some ions with no effect on water and other with a marginal effect. Importantly, these results did not follow the ordering of the Hofmeister series.[36] Computationally, molecular dynamics is often employed because of the structural and dynamical insights provided. For instance, molecular dynamics simulations have been used to observe the partitioning of the ion between the bulk and air-water interface,[6,37] to measure tetrahedrality in the solvation shell (as a measure of order),[38] to count the average number of hydrogen bonds,[39] to examine the patterning and order of solvation shells using the pair correlation function,[40–42] and to calculate water reorientation time and ion-water hydrogen bonding lifetime using the velocity autocorrelation function.[41,43] Importantly, by using these different metrics and interpretations of "structure-making" properties, different conclusions have been reached regarding the ion's "structure-making" or "disorder-making" ability.

Despite these strides in understanding the Hofmeister effect, a general theory that unifies the observations listed above is far from being complete. Although the Hofmeister series was developed originally to track the effect of the ions in the salting-in and salting-out of proteins in an aqueous solution, recent literature may have implied that the ions (without the protein) may affect the long-range structure of liquid water depending on where they reside in the series.[23,24,28–32,44] Here, as a new perspective in the effort to gain molecular level insight into the Hofmeister effect, *ab initio* electronic structure calculations for aqueous ionic clusters were used to analyze the effect of various cations and anions on either side of the Hofmeister series (1) on the interactions between water molecules in the immediate surrounding of these ions. We selected aqueous ionic clusters containing singly and doubly charged cations and anions residing on the

two opposite ends of the Hofmeister series to be able to investigate the effect of both the charge (nominal value, sign) and structure making/breaking ability of the ion on the interactions of the surrounding hydrogen bonded water network. We obtained cluster minima of the kosmotropes, Ca^{2+} and SO_4^{2-}, and chaotropes, NH_4^+ and ClO_4^-, with 9 water molecules and performed a many-body expansion (MBE) of the ion-water and water-water interactions in order to be able to directly compare the results with the ones previously reported for pure water[45] and monatomic alkali metal / halide aqueous clusters[46] with the same number of fragments. As in our previous study, for each ion we considered two structural arrangements: one with the ion located inside, the other on the outside of a water cluster network. This choice of cluster size was deemed large enough to describe artifacts due to BSSE and it can produce realistic conformations mimicking fully solvated (ion inside) and interfacial (ion outside) solvation, while at the same time being computationally tractable.

The MBE, a combinatorial approach, was used to partition the binding energy of the system into its constituent n-body terms[47–49] where the "fragments" or "bodies" (B) refer to the individual water molecules and ions.

$$D_{e,cluster} = \sum \Delta E_I + \sum \Delta E_{IJ} + \sum \Delta E_{IJK} + \cdots + \sum \Delta E_{IJK\ldots N} \qquad (2)$$

The 1-B term (ΔE_I) is the energetic penalty[50,51] for each fragment to deform from its gas-phase geometry to the one it adopts in the cluster geometry due to its interaction with the rest of the "bodies". The 2-B term (ΔE_{IJ}) is typically the largest energetically favorable term that reflects the difference between each dimer energy and the energy of the monomers that comprise the dimer. The 3-B term (ΔE_{IJK}) describes how the energy of each dimer and monomer is perturbed with respect to the other monomers present in the system. The successively higher order terms are defined analogously and tend to decrease in magnitude in hydrogen-bonded systems.[52,53]

This type of energy analysis has been recently applied to pure water clusters of varying sizes[45] as well as monatomic (alkali metal cation and halide anion) aqueous clusters[46]. It was shown that the MBE of pure water clusters converges at the 4-B term while the MBE of monatomic cations/anions is comprised of especially large 2-B interactions with a repulsive 3-B term, in contrast to the pure water clusters, which exhibit an attractive 3-B term at the cluster minima

considered in these previous studies. In addition, an unexpected linear anti-correlation between the total 2-B ion-water and the total 2-B water-water interaction was observed for both the alkali metal cation and the halide anion clusters. The MBE of Hofmeister ion aqueous clusters, to the best of our knowledge not reported to date, contributes a novel perspective to the discussion of the Hofmeister effect by breaking down the energetics of the whole system, analyzing the ways and the extent that a specific ion impacts these interactions, and comparing this breakdown to the one for ions in a different position of the Hofmeister series. Furthermore, the effect of the cations/anions and kosmotropes/chaotropes on the interactions of the surrounding water molecules can be assessed independently. Being able to examine the physics of one ion at a time is a useful way to reduce the problem, since it has been shown that pairs of ions often lead to different behaviors due to solvent separated, solvent shared, and contact ion pairing.[54,55] In addition, the relative impact of cations and anions[26,41,56] has also been discussed. By studying each independently, differences in the energetics of cationic and anionic systems can be analyzed and quantified. To the best of our knowledge, this type of energy analysis has not been reported earlier for these systems. The paper is organized as follows: in Section II we outline the computational details and a brief overview of the methodology we adopted in our theoretical study. In Section III we present the results for the magnitude of the various many-body (MB) interactions and the contribution of the constituent ion-water (I-W) and water-water (W-W) interactions. We further attempt to identify correlations between the total (I-W) and (W-W) interactions in an effort to investigate how ions on different ends of the Hofmeister series (chaotropes/kosmotropes) affect the W-W interaction. In that section we also investigate the profile of the 2-B (I-W) BSSE correction as a function of the interfragment distance for the different ions in an effort to integrate the current results with the ones previously reported for (W-W) and alkali metal / halide – water interactions.[45,46]

II. Computational Details

The kosmotropes Ca^{2+} and SO_4^{2-} and chaotropes NH_4^+ and ClO_4^- ions were studied as part of water clusters containing nine water molecules. Note that these singly and doubly charged ions reside close to the opposite ends of the Hofmeister series (1) for both cations and anions. The size of these clusters (ion plus 9 water molecules) was selected because it was large enough to allow

forming configurations in which the ion resides both in the inside and the outside of a water network and allows for a direct comparison of the results with pure water clusters and monatomic aqueous clusters of the same size[45,46]. The intent is to initially investigate the dependence of the results on the different conformational isomers and coordination numbers, albeit with this limited sampling of the configuration space that explores "bulk-like" and "interface-like" environments. The same number of "bodies" (10) was used in order to directly compare the current results with previous ones for the $(H_2O)_{10}$ and $Z^{+}(H_2O)_9$, Z=Li, Na, K, Rb, Cs, F, Cl, Br, I, clusters.

Some of these structures were taken from published works[57–60] and, when not available in the literature, were built from a z-matrix. The $NH_4^+(H_2O)_9$ structure with the ion on the inside was built entirely from a z-matrix, constraining dihedral angles of 120º and tetrahedral binding angles of 109.5º to keep the ion on the inside of the cluster. The remaining structures are local minima on the potential energy surface. The structures of the clusters analyzed via the MBE are shown in Figure 1 and their Cartesian coordinates are included in the Supporting Information (SI).

The MBE, equation (2), was carried out to the 10th order (1,024 energies computed) for each cluster, viz.

$$D_{e,cluster} = \sum_{I}^{10} \Delta E_I + \sum_{I<J}^{10} \Delta E_{IJ} + \sum_{I<J<K}^{10} \Delta E_{IJK} + \cdots + \sum_{I<J<K<\cdots<n}^{10} \Delta E_{IJK\ldots N} \qquad (3)$$

The 1-body term (4) is the molecular relaxation term describing the energetic difference between the monomers in the cluster geometry relative to the reference (relaxed) geometry:

$$\Delta E_I = E_I - E_{I,ref} \qquad (4)$$

The two-body term (5) is the energetic difference between each dimer and the monomers that comprise the dimer:

$$\Delta E_{IJ} = E_{IJ} - E_I - E_J \qquad (5)$$

The three-body term (6) is defined as energy difference between each trimer and the monomers comprising that trimer while also considering the lower order n-body terms (2-body terms of each dimer that makes up the trimer):

$$\Delta E_{IJK} = E_{IJK} - \Delta E_{IJ} - \Delta E_{IK} - \Delta E_{JK} - E_I - E_J - E_K \qquad (6)$$

The higher order terms (4- to 10-B) in the expansion are defined analogously.

All calculations were performed at the MP2 level with the aug-cc-pVDZ basis set[61] for all atoms except calcium, for which the Stuttgart RSC 1997 ECP[62] was used. Importantly, the resulting *n*-body terms of the MBE were corrected for the basis set superposition error (BSSE) (additional 1,023 energies for the various fragments in the full cluster basis for each ion and inside/outside configuration considered), which is the result of the artificial lowering of the energy of the complex due to borrowing of basis functions from other fragments in proximity. This effect is present in all binding energy calculations and, ultimately, is an artifact of an incomplete, finite basis set. We correct for BSSE using the function counterpoise correction as outlined by Boys and Bernardi.[63] During our earlier studies,[45,46] it was shown that the MP2/aug-cc-pVDZ calculations sufficiently describe the values of the 3-B, 4-B and higher terms at the complete basis set (CBS) limit when BSSE corrections are taken into account.[45,46] Naturally the 2-B term and, in turn, the total cluster binding energy (whose largest component is the former) are not converged at that level; however, the focus of the present study is in the magnitude of the higher order terms and their correlations, which are accurately accounted for. The MBE for the $Ca^{2+}(H_2O)_9$ clusters was also performed with the aug-cc-pVTZ basis set up to the 6-body term to ensure that the behavior of the MBE with basis set for an ionic cluster encompassing a doubly charged cation follows the same pattern as for a monatomic (positive or negative) ion. The calculations were performed with zero linear dependencies to guarantee that the full number of basis functions were utilized. All calculations were performed with the NWChem 6.8 electronic structure package.[64]

III. Results and Discussion

a. Magnitude of Many-Body (MB) Terms

We first investigate the behavior of the MBE for a doubly charged ion, since this is the first instance that we attempt a decomposition for such a system. For the two isomers (ion inside and ion outside) of the $Ca^{2+}(H_2O)_9$ cluster (cf. Figure 1) the MBE was performed at the MP2 level up to the (complete) 10^{th} order with the aVDZ basis set and up to the 6^{th} order with the aVTZ basis set. The BSSE-corrected results with these two basis sets are summarized in Table 1. The BSSE-corrected MP2 1-B to 6-B terms are plotted in Figure 2 with the aVDZ (blue) and aVTZ (orange)

basis sets. At this point we are interested in the basis set dependence of the various terms and we will discuss the differences in the magnitudes of the individual terms between the two isomers later. There is no significant qualitative difference in the resulting MB terms between these two basis sets. There is a noteworthy quantitative difference in the 2-body term with the largest difference between the calculated MB terms with different basis set sizes being 8.8 kcal/mol. This is consistent with work reported earlier[46] on the monatomic aqueous clusters, utilizing basis set sizes up to the aug-cc-pV5Z. From these results we ascertain that the MBE for an aqueous doubly charged ion behaves similarly to the one for a singly charged one and this result further justifies the level of theory and protocol (MP2/aVDZ including BSSE corrections) we have adopted for the MBE analysis in this study.

The magnitude of the various MBE terms (in kcal/mol) up to the 10th order for the ion inside and ion outside isomers of the four ionic clusters considered in this study (cf. Figure 1) at the MP2/aVDZ level of theory including BSSE corrections are listed in Table 2 (see Table TS1 of the SI for the BSSE-uncorrected values). The numbers in parentheses in Table 2 correspond to the percentage contribution of each term to the total cluster binding energy. These results suggest that terms above the 4-B (save the ion inside isomer of the $Ca^{2+}(H_2O)_9$ cluster) are negligible, contributing < 0.3% to the total binding energy. The BSSE-corrected many-body terms of $(H_2O)_{10}$ will be used as a reference,[45] providing a direct point of comparison in this section. The full MBE of the aqueous ionic clusters $Ca^{2+}(H_2O)_9$, $NH_4^+(H_2O)_9$, $SO_4^{2-}(H_2O)_9$, $ClO_4^-(H_2O)_9$ and the $(H_2O)_{10}$ water cluster are collected together in Figure 3. The aqueous ionic clusters exhibit an increased 2-B term relative to that of pure water due to the strong ion-water (charge-dipole) interaction, which is naturally larger for the divalent ions. This is consistent with what was observed with the MB expansion of water clusters containing monatomic ions.[46] The percentage contribution of the 2-B term to the total cluster binding energy is noticeably larger for the kosmotropes (calcium and sulfate) than the chaotropes (perchlorate and ammonium). This is not surprising given that kosmotropes are typically more charge dense[65–69] and the 2-B terms are dominated by the charge-dipole interactions between the ion and water. Figure 4 shows the individual 2-B (I-W) contributions to the total BSSE correction for the various ions considered in this study as a function of $q \cdot \cos(\theta)/R_{X-O}^2$, where q is the magnitude of the charge, R is the distance and θ the angle between the ion and the molecular dipole of the nearest water molecule. The 72 points follow a linear trend (broken line) with slope -1.556 quite closely (R^2 = 0.9777). When these interactions

are not scaled for the total charge (i.e., the x-axis is just $\cos(\theta)/R_{X-O}^2$), two linear trends emerge for the $q = \pm 1$ and $q = \pm 2$ cases (see Figure FS1 in the SI). The 2-B terms are larger when the ion is on the inside because the ion-water distances are, on average, shorter for this cluster configuration thus resulting in stronger charge-dipole interactions. Despite the large magnitude of the attractive 2-B terms, the 3-B terms of the aqueous systems are repulsive with the exception of perchlorate and ammonium on the outside of the cluster. This contrasts the attractive 3-B term for pure water clusters, which further strengthens the hydrogen bonding network. The two kosmotropes (calcium and sulfate) have a large repulsive 3-B term, which becomes increasingly more favorable as the ion becomes more chaotropic, with perchlorate and ammonium exhibiting a favorable 3-B term when these ions are located on the outside of the cluster. The 4-B term varies significantly based on the location of the ion in the water cluster and may depend on the sign of the ionic charge (anion or cation). When the ions are located on the inside, the kosmotropes exhibit an increased favorability of the 4-B term relative to pure water, the perchlorate anion behaves similarly to pure water, whereas the ammonium cation has a slightly repulsive term. However, when the ion resides on the outside of the cluster, the 4-B term is weakly attractive for all ions, save calcium. The anions have a consistently favorable 4-B term, while the cations have a strongly attractive or repulsive term depending on its location in the cluster. The 4-B term of chaotropes are noticeably more negative when the ions reside on the outside of the cluster. The opposite is true for the kosmotrope ions considered in this study.

The expansion of the pure water cluster converges at the 4-B term.[45] However, the expansions of the aqueous clusters extend beyond the 4-B term, to varying degrees. Notably, calcium, when located on the inside of the cluster, exhibits a 5-B term of 6.07 kcal/mol (2.1% or the total cluster binding energy) and a 6-B term of -1.00 kcal/mol (0.3% of the total cluster binding energy). Conversely, ammonium has a small 5-B term of -0.15 kcal/mol (0.1%) and just -0.05 kcal/mol when residing on the inside and outside of the aqueous cluster, respectively. The 5-B term of ammonium is noteworthy, but not nearly as significant as the one for the two kosmotropes. In general, the MBE appears to converge more quickly for the chaotropes than for the kosmotropes. Further, when the ion is on the inside of the cluster, the MBE tends to have larger higher order terms in the expansion. This is likely due to increased proximity of the ion to the water molecules, resulting in stronger (I-W) interactions and a further disruption and subsequent weakening of the

(W-W) interaction. Considering the MB terms altogether, the expansion of the chaotropic ions more closely resembles that of pure water than the kosmotropes do.

Examining the total magnitude of the MB terms provides valuable insight, as discussed previously. However, other variables such as geometry and coordination number likely play a role, making it difficult to extract general trends solely by examining the many-body terms. The subsequent sections aim at dissecting the MB terms in order to provide a better understanding of the ion's role in affecting these MB terms and how the (W-W) interactions are impacted as a result of the ion's presence.

b. Ion-Water (I-W) and Water-Water (W-W) Contributions to the MBE Terms

In this section we examine the contribution of the total (I-W) and (W-W) interactions to the total binding energy as well as to the individual MB terms. Each term in the MBE can be split into these two contributions as:

$$D_e = \sum \Delta E_I + \sum \Delta E_W + \sum \Delta E_{I-W} + \sum \Delta E_{W-W} + \sum \Delta E_{I-W-W} + \sum \Delta E_{W-W-W} + \cdots \quad (7)$$

The total (I-W) and (W-W) interactions are the sums of the corresponding terms from each term in the MBE. Table 3 lists the total (I-W) and (W-W) interactions as well as their contributions to the individual 1-B to 10-B terms for the two configurations (ion inside / ion outside) of the four ions considered in this study. The numbers in parentheses indicate the percentage contributions of each term [(I-W) and (W-W)] to either the total cluster binding energy or to the individual MB terms from 1-B to 10-B (the two numbers in parentheses add up to 100% for each MB term as well as the total).

Composition of the Total Binding Energy: The total (I-W) and (W-W) interactions and their variation for each ion are shown in Figure 5 (note that their sum is the total binding energy for each cluster). Importantly, the cations and anions are separated, ensuring that only ions of the same sign are compared to one another depending on their position in the Hofmeister series (1). Within the cation (left) and anion (right) sections of the plot, the leftmost ions are the kosmotropes (Ca^{2+}, SO_4^{2-}) and the rightmost ions are the chaotropes (NH_4^+, ClO_4^-). The open circles denote the results when the ion is on the outside of the cluster whereas the closed circles the ones when the ion is in the inside. Figure 5 clearly demonstrates the anti-correlation between the (I-W) and (W-W)

interactions, previously reported for the alkali metal and halide aqueous clusters: the stronger the (I-W), the weaker the (W-W) interaction. It is important to point out that the kosmotropes considered in this study have significantly larger total binding energies than the corresponding chaotropes, due to the difference in the magnitude of the charge ($q = \pm 2$ vs. $q = \pm 1$). However, even within the doubly charged kosmotropes (Ca^{2+}, SO_4^{2-}), the stronger (I-W) interaction (in Ca^{2+}) results in a weaker (W-W) interaction, whereas the weaker (I-W) interaction (in SO_4^{2-}) results in a slightly stronger (W-W) interaction than for Ca^{2+}. The same trend, albeit not as pronounced as in the kosmotropes, in observed for the chaotropes. For the kosmotropes, the binding energy is largely described by the (I-W) interactions since these amount from 89% to 106% of the total cluster binding energy. However, for the chaotropes the (W-W) interaction comprises a much larger percentage (55% to 95%, cf. Table 3) of the total cluster binding energy. Furthermore, the (I-W) interactions vary more significantly than the (W-W) interactions based on the identity of the ion. This is interesting because the ion identity affects the (W-W) interactions to a smaller degree than one would expect based on the total MB terms. Understanding these contributions to the individual many-body terms will be the subject of the following two sections.

Composition of Individual MB Terms: In this section we discuss the contributions of the (I-W) and (W-W) interactions to the individual 1-B to 10-B terms, which are listed in Table 3. The 2-B to 4-B interactions are the primary focus because they are the largest contributors to the total binding energy. Figure 6 shows the individual ion-water (left panel) and water-water (right panel) contributions to the 2-B to 4-B terms for the kosmotropic (left panels within each plot) and the chaotropic ions (right panels within each plot) plotted according to the convention used for Figure 5. Open circles represent the values calculated when the ion is on the outside whereas closed circles represent the values for the clusters with the ion on the inside of the cluster.

We first examine the ion-water terms (left panel of Figure 6). The variation of the ion-water terms is more regular than the water-water terms. Indeed, the individual (I-W), (I-W-W) and (I-W-W-W) terms oscillate in sign with their magnitude being larger for the kosmotropic ions. However, we see a more consistent trend in the 4-B (I-W-W-W) term than in the total 4-B term. The 4-B term is relatively large and favorable (attractive) for the kosmotropes, while it is practically zero for the chaotropes. Interestingly, the 4-B terms for all systems with the ion on the outside, remain relatively close to zero. The 3-B and 4-B terms for the chaotropes approach zero, leaving the majority of the ion-water contributions described by the 2-B term. Most significantly,

the 3-B (I-W-W) term for the ammonium systems does not exceed 4.2 kcal/mol whereas that of the calcium system is greater than 100 kcal/mol. Further, the kosmotropes, particularly calcium, exhibits higher order ion-water terms, extending up to a 6-B term that is ~1 kcal/mol. In general, the ion-water contributions are much smaller when the ion resides on the outside of the aqueous cluster. Since the ion is, on average, located farther from the water molecules, this result is expected.

In regards to the water-water contributions in the MBE (right panel of Figure 6), they are more favorable for the chaotropes for each term examined (2-B to 4-B). This is consistent with the increased percentage contribution of the water-water interaction to the total cluster binding energy discussed in the previous subsection for the chaotropes. The water-water contributions are much closer to zero for the kosmotropes, reflecting a dominance of the ion-water interaction in nearly all terms of the MBE. The convergence of the water-water contributions of these aqueous clusters is similar to that for the pure water clusters, which converges at the 4-body term. However, in terms of the magnitude and sign of the terms, there are considerable differences. When the chaotropes are on the outside of the cluster, the MBE exhibits water-water 2- to 4-B body terms that resemble that of pure water. For comparison, the 2-, 3-, and 4-B terms of water are -62.76 (76.2%), -21.69 (26.3%) and -1.97 (2.4%) kcal/mol, while those of ammonium on the outside of the cluster are -42.44 (79.0%), -12.86 (23.9%) and -1.40 (2.6%) kcal/mol and perchlorate are -29.76 (80.0%), -8.80 (23.7%) and -0.49 (1.3%) kcal/mol, respectively. All other ionic clusters exhibit at least one of the 2- to 4-B terms that is energetically unfavorable. Interestingly, when the chaotropes are on the inside and the kosmotropes are on the outside, the water-water terms are similar. When the ion is in the center of the cluster, we would expect maximal disruption of hydrogen bonding. Thus, the chaotropes disrupt the hydrogen bonding network when in the inside in a similar manner as when the kosmotropes are on the outside. Further, we notice that strong kosmotropes perturb the water-water many-body terms differently. Calcium on the inside, has repulsive 2-B and 4-B terms, while sulfate only has a repulsive 4-B term. The fact that calcium has a repulsive water-water 2-B term originates from the strong structuring of the water molecules in the first solvation shell around the ion resulting in the majority of the water dimers to be unfavorably oriented with the oxygen atoms (lone pairs) facing one another. Importantly, none of these aqueous clusters exhibit stronger water-water interactions than the pure water clusters. These results suggest that all ions weaken the water-water interactions, likely in their varying ability to

orient nearby water molecules around themselves. The amount that they are impacted, however, depends on the identity of the ion. Kosmotropic ions exhibit weaker water-water interactions than chaotropic ones (see also the discussion about the anti-correlation between (I-W) and (W-W) interactions in the previous subsection).

c. Trends in the MBE Terms Across the Hofmeister Series

By combining the results of the present study with those reported earlier for the monatomic alkali metal and halide ionic aqueous clusters,[46] we can examine the variation of the different MBE terms across the Hofmeister series. Figure 7 depicts the variation of the 2- to 4-B ion-water interactions for the cations (left panel) and anions (right panel) across the Hofmeister series (1). The corresponding plot for the water-water interaction is shown in Figure 8 for the cations (left panel) and anions (right panel). Both Figures are drawn using the same plotting conventions as in Figure 5. The ion-water 2-B, 3-B and 4-B terms decrease in magnitude (the last two towards zero) when going from the kosmotropes to the chaotropes for both the cation and anion series (Figure 7). Specifically, the 3-B and 4-B terms decrease in magnitude (toward zero) as the center of the Hofmeister series is approached (K^+ and Cl^-). However, there is no discernable difference between the ions in the center of the Hofmeister series and the chaotropes by looking at solely the ion-water contributions. All these ions have small 3-B and 4-B terms with similarly large 2-B terms.

In contrast, the trends are not as smooth for the water-water interactions (Figure 8). Upon comparing the water-water interaction for ions located in the middle of the Hofmeister series in Figure 8, we notice different behaviors for the cations and anions. Anions, especially the halides, tend to have weaker water-water interactions than the corresponding cations (Li^+, Na^+, K^+). Additionally, each monatomic ion has a favorable (attractive) 3-B term for configurations having the anion on the outside and the cation in the inside. However, this pattern does not extend to the polyatomic ions considered in the present study. Further, we see an increase in favorability of the water-water interactions from the kosmotropes to the chaotropes. While that trend exists in the anions, the difference between the ions is relatively small. The Hofmeister cations calcium and ammonium generally exhibiting the most extreme behavior.

Figures 9 and 10 show correlation plots between (I-W), (W-W), (I-W-W), and (W-W-W) interactions for the aqueous clusters in this study and includes the results for the monatomic

aqueous clusters reported earlier.[46] While the alkali metals and halide ion-water clusters exhibit clear trends (indicated by the solid lines) for each set of plots, the only Hofmeister ion that fits with these established trends is calcium. Since calcium is also a monatomic ion like the alkali metal and halide ions, it is likely that the difference in hydrogen bonding character between monatomic and polyatomic ions complicates these correlations. Despite the polyatomic and monatomic ions not fitting on the same linear trend, we still see a consistent general anticorrelation between the (I-W-W) vs. (I-W) interactions. The ion systems with the strongest (I-W) interactions have the most repulsive (I-W-W) terms. This appears to be a quintessential characteristic of these aqueous clusters, independent of ion identity. Interestingly, ammonium often exhibits the opposite trend as the rest of the cations, viz. the point representing the interactions for the ion on the outside more closely fits the trend for the other ions when on the inside and vice versa. This is true for all correlation plots with the exception of (W-W) vs. (I-W). A further study including more ions in the Hofmeister series is warranted.

d. Profile of 2-Body BSSE Corrections

As mentioned earlier, BSSE corrections are important for a more accurate description of the terms in the MBE. Heindel and Xantheas[45,46] have previously reported that the 2-B contribution to the total BSSE correction is the most substantial and have suggested an analytic formula for its estimate based on the distance between the fragments via a fit to an error function:

$$\Delta E_{2B-BSSE} = a\left[1 + erf(-b \cdot R_{ij})\right] \quad (8)$$

where a and b are empirical parameters and R_{ij} is the distance between the fragments (oxygen-oxygen or ion-oxygen distance).

Figure 11 shows the 2-B contribution to the total BSSE correction profile versus the distance between fragments (taken as either as the ion-oxygen or the oxygen-oxygen distance) for the ions considered in this study (except calcium), the halide ions,[46] and pure water clusters.[45] Note that this is for 498 water dimer and 108 ion-water pairs (for the aqueous clusters of the Cl^-, Br^-, I^-, SO_4^{2-}, ClO_4^- and NH_4^+ ions), which have been evaluated in the full cluster basis to account for the 2-B contribution to the total BSSE. As in our earlier study,[46] the *x*- and *y*-axes are scaled[70–72] by the values of the gas phase dimer (ion-water or water-water) equilibrium distance and BSSE

correction of the binding energy, respectively. The scaled 2-B BSSE corrections for the various aqueous systems, except Calcium, follow a decaying trend with the scaled intermolecular distances that fits quite well to equation (8) (a = 14.61, b = 1.30, R^2 = 0.9856), as displayed by the solid line in Figure 11. Calcium was excluded from Figure 11 because it exhibits a 2-B BSSE profile that decays to zero more rapidly than the other ions as the distance between pairs of molecules increases, behaving similarly to $Li^+(H_2O)_9$.[46] The corresponding profiles for the unscaled energies / distances for each individual cluster are shown in Figure FS2 in the SI; the individual fits to equation (8) are listed in Table TS3 of the SI.

IV. Conclusions

The effect of the Hofmeister ions on the structure of the solvent is an active topic in physical chemistry research. In an effort to provide a quantitative understanding of how ions in the Hofmeister series affect the interaction between surrounding water molecules we have performed a MBE analysis using aqueous ionic clusters as models. We have examined aqueous clusters of both anionic and cationic kosmotropes (Ca^{2+} and SO_4^{2-}) and chaotropes (NH_4^+ and ClO_4^-) with 9 water molecules to compare with previous water, alkali metal and halide aqueous clusters of the same size. The alkali metals and halide ion-water MBE analysis reported previously have been useful data for comparison, given that those ions are located in the middle of the Hofmeister series. In agreement with our previous results for these other systems we have found that the MBE converges to practically the 3-B term, with terms above the 4-B being negligible, contributing < 0.3% to the cluster binding energy. As observed in monatomic aqueous systems,[46] the 2-B term in the expansion is accentuated relative to that of pure water, even more so with kosmotropes. Similarly, the 3-B term is repulsive, in contrast to pure water clusters, with the exception of chaotropes residing on the outside of the water cluster. The expansion of the kosmotropic systems, in general, are largely dominated by the ion's contributions to the many-body terms with the (W-W) terms lying relatively close to zero. In contrast, the chaotropic systems, exhibiting much weaker (I-W) interactions, had more significant contributions from water-water interactions but not surpassing those found in a pure water cluster.[45] This prominent anticorrelation between (I-W) and (W-W) interactions suggests that kosmotropes, which exhibit stronger (I-W) interactions, sacrifice the favorability of the water-water interactions, likely by preferentially orienting the water

molecules around the ion to maximize the ion-water interactions. Further, systems with stronger ion-water interactions tend to have larger higher-order terms in the many-body expansion. This aligns with what has been previously reported for the $Li^+(H_2O)_9$ system.[46] The expansion of chaotropic systems, exhibiting relatively weak ion-water interactions, converges more quickly and more closely resembles that of water.

Interestingly, the expansion of kosmotropic systems on the outside looks very similar to that of chaotropic systems on the inside of the cluster. Since (I-W) interactions are smaller when the ion is on the outside of the cluster, this demonstrates that kosmotropes and chaotropes interact in a similar way with water. However, due to their difference in (I-W) interactions, kosmotropes have an increased ability to diminish water-water interactions, which is evident when the ion is centrally located in the cluster. When the chaotropes reside on the outside of the cluster, the expansion more closely resembled that of pure water. Importantly, there is no evidence suggesting that water-water interactions are enhanced in the presence of either kosmotropic or chaotropic ions. Rather, the many-body expansion of increasingly chaotropic ions approaches the behavior of water, as the ion presents a weaker influence on the surrounding water molecules. This is true both for the water-water contributions and the overall many-body terms. These results suggest that all ions disrupt and weaken water-water hydrogen bonding in the short-range. These observations are consistent with other experimental and theoretical work supporting a relatively local disruption or weakening of hydrogen bonds.[33,66,69,73,74]

Lastly, we found that the 2-B contribution to the total BSSE correction profile with intermolecular separation follows the trend (R^2=0.9856) reported previously for water, alkali metal and halide aqueous clusters.[45,46] However, as previously observed for some other alkali metal ion-water systems, namely $Li^+(H_2O)_9$, the 2-B BSSE profile for calcium decays more rapidly with the distance between the ion and water molecule increases. While some of the monatomic cations have a different profile, ammonium aligns quite well with the anion-water and pure water clusters.

The MBE expansion for aqueous ionic clusters is more complex than the pure water clusters and converges at different ranks of the expansion depending on the identity of the ion and its position within a water network. This is consistent with the fact that the development of ab-initio based, many-body polarizable ion-water classical potentials[75,76] has not yet attained the accuracy of the pure water potentials[77] developed with the same fitting protocol to ab-initio results.

The static cluster configurations used as models in this study, naturally fail to capture any dynamical effects that kosmotropes and chaotropes may impart upon the surrounding hydrogen bonding network. Nevertheless, they provide the stepping-stone for future studies that will examine the effect of geometric conformations and temperature effects on the magnitude of the respective MBE terms for those systems. A more detailed and quantitative analysis of the structural patterns induced by the disparate MB interactions of these different ions is warranted as it can provide a useful perspective into the elusive Hofmeister effect.

Acknowledgment: K.M.H. acknowledges support from the Mickey and Karen Schurr Endowed Fund and J.P.H. acknowledges support from the Norman and Lillian Gregory Endowed Fund in Chemistry at the University of Washington. This work was supported from the Center for Scalable Predictive methods for Excitations and Correlated phenomena (SPEC), which is funded by the U.S. Department of Energy, Office of Science, Basic Energy Sciences, Chemical Sciences, Geosciences and Biosciences Division, as part of the Computational Chemical Sciences Program at Pacific Northwest National Laboratory. Pacific Northwest National Laboratory (PNNL) is a multi-program national laboratory operated for DOE by Battelle. This research also used resources of the National Energy Research Scientific Computing Center, which is supported by the Office of Science of the U.S. Department of Energy under Contract No. DE-AC02-05CH11231.

ASSOCIATED CONTENT

Supporting Information. Cartesian coordinates of all cluster configurations, 2-B ion-water charge-dipole interactions, unscaled 2-B contributions to the total BSSE correction, and magnitude of BSSE-uncorrected MB terms at the MP2/aVDZ level of theory.

Table 1. Basis set dependence of the MBE terms up to 6-B for the $Ca^{2+}(H_2O)_9$ clusters at the MP2 level with the aVDZ and aVTZ basis sets including BSSE corrections.

	Ion inside		**Ion outside**	
k	MP2/aVDZ	MP2/aVTZ	MP2/aVDZ	MP2/aVTZ
1-B	0.80	0.88	3.416	3.837
2-B	-379.547	-387.367	-294.908	-303.757
3-B	104.649	107.794	18.935	21.050
4-B	-26.580	-27.612	0.879	0.581
5-B	6.074	6.378	-0.411	-0.370
6-B	-0.996	-1.070	0.133	0.136

Table 2. MBE (kcal/mol) terms for the various isomers of the clusters in Figure 1 at the MP2/aVDZ level of theory including BSSE corrections. The numbers in parentheses correspond to the percentage of the total energy. The uncorrected values are provided in the SI.

	$Ca^{2+}(H_2O)_9$		$NH_4^+(H_2O)_9$		$SO_4^{2-}(H_2O)_9$		$ClO_4^-(H_2O)_9$	
k	**Ion inside**	**Ion outside**	**Ion inside**	**Ion outside**	**Ion inside**	**Ion outside**	**Ion inside**	**Ion outside**
1-B	0.81 (-0.3)	3.42 (-1.3)	0.41 (-0.4)	3.82 (-3.2)	3.24 (-1.8)	5.11 (-2.9)	1.08 (-1.2)	2.58 (-2.7)
2-B	-379.55 (128.4)	-294.91 (108.4)	-111.40 (106.5)	-111.97 (94.9)	-215.42 (120.5)	-193.41 (110.9)	-96.76 (108.7)	-94.30 (99.1)
3-B	104.65 (-35.4)	18.94 (-7.0)	4.74 (-4.5)	-8.65 (7.3)	38.73 (-21.7)	14.84 (-8.5)	8.36 (-9.4)	-2.80 (2.9)
4-B	-26.58 (9.0)	0.88 (-0.3)	1.80 (-1.7)	-1.15 (1.0)	-5.70 (3.2)	-1.01 (0.6)	-1.95 (2.2)	-0.68 (0.7)
5-B	6.07 (-2.1)	-0.41 (0.2)	-0.15 (0.1)	-0.05 (0.0)	0.30 (-0.2)	0.10 (-0.1)	0.27 (-0.3)	0.10 (-0.1)
6-B	-1.00 (0.3)	0.13 (-0.0)	-0.001 (0.0)	0.04 (0.0)	0.11 (-0.1)	-0.01 (0.0)	-0.03 (0.0)	-0.003 (0.0)
7-B	0.07 (-0.0)	-0.05 (0.0)	0.001 (0.0)	-0.01 (0.0)	-0.04 (0.0)	0.000 (0.0)	0.003 (0.0)	0.000 (0.0)
8-B	0.01 (0.0)	0.01 (0.0)	0.000 (0.0)	0.000 (0.0)	0.01 (0.0)	0.000 (0.0)	0.000 (0.0)	0.000 (0.0)
9-B	-0.002 (0.0)	0.000 (0.0)	0.000 (0.0)	0.000 (0.0)	-0.001 (0.0)	0.000 (0.0)	0.000 (0.0)	0.000 (0.0)
10-B	0.002 (0.0)	0.000 (0.0)	0.000 (0.0)	0.000 (0.0)	0.000 (0.0)	0.000 (0.0)	0.000 (0.0)	0.000 (0.0)
Total	**-295.52**	**-272.00**	**-104.60**	**-117.97**	**-178.77**	**-174.38**	**-89.03**	**-95.11**

Table 3. Decomposition of the MBE (1-B to 10-B) terms into ion-water (I-W-…-W) and water-water (W-W-…-W) contributions (kcal/mol) for the clusters of Figure 1 at the MP2/aVDZ level of theory including BSSE corrections. Parentheses indicate the percentage of each contribution to the total magnitude of the MB terms listed in Table 2. The uncorrected values are provided in the SI.

	$Ca^{2+}(H_2O)_9$				$NH_4^+(H_2O)_9$			
	Ion inside		**Ion outside**		**Ion inside**		**Ion outside**	
k	**I-W**	**W-W**	**I-W**	**W-W**	**I-W**	**W-W**	**I-W**	**W-W**
1-B	0.00 (0.0)	0.81 (100.0)	0.00 (0.0)	3.42 (100.0)	0.13 (32.4)	0.28 (67.7)	0.88 (22.9)	2.95 (77.1)
2-B	-398.78 (105.1)	19.23 (-5.1)	-284.61 (96.5)	-10.30 (3.5)	-103.21 (92.7)	-8.18 (7.4)	-69.55 (62.1)	-42.43 (37.9)
3-B	106.76 (102.0)	-2.11 (-2.0)	16.34 (86.3)	2.59 (13.7)	1.63 (34.4)	3.11 (65.6)	4.21 (-48.6)	-12.86 (148.6)
4-B	-26.96 (101.4)	0.38 (-1.4)	0.73 (82.8)	0.15 (17.3)	1.76 (97.8)	0.04 (2.2)	0.26 (-22.2)	-1.40 (122.2)
5-B	6.08 (100.1)	-0.01 (-0.1)	-0.41 (100.9)	0.004 (-0.9)	-0.14 (91.3)	-0.01 (8.7)	-0.05	0.007
6-B	-0.99 (99.1)	-0.008 (0.9)	0.14 (103.2)	-0.004 (-3.2)	-0.001	0.000	0.03	0.009
7-B	0.06	0.002	-0.05	0.000	0.001	0.000	-0.006	0.001
8-B	0.01	0.000	0.01	0.000	0.000	0.000	0.000	0.000
9-B	-0.002	0.000	0.000	0.000	0.000	0.000	0.000	0.000
10-B	0.002	0.000	0.000	0.000	0.000	0.000	0.000	0.000
Total	**-313.82 (106.2)**	**18.30 (-6.2)**	**-267.86 (98.5)**	**-4.14 (1.5)**	**-99.83 (95.4)**	**-4.77 (4.6)**	**-64.24 (54.5)**	**-53.73 (45.5)**

	$SO_4^{2-}(H_2O)_9$				$ClO_4^-(H_2O)_9$			
	Ion inside		**Ion outside**		**Ion inside**		**Ion outside**	
k	**I-W**	**W-W**	**I-W**	**W-W**	**I-W**	**W-W**	**I-W**	**W-W**
1-B	0.58 (17.9)	2.66 (82.1)	0.93 (18.3)	4.18 (81.8)	0.11 (10.4)	0.96 (89.6)	0.76 (29.4)	1.82 (70.6)
2-B	-210.22 (97.6)	-5.20 (2.4)	-174.71 (90.3)	-18.71 (9.7)	-82.93 (85.7)	-13.83 (14.3)	-64.54 (68.4)	-29.76 (31.6)
3-B	46.00 (118.8)	-7.27 (-18.8)	19.46 (131.1)	-4.62 (-31.1)	15.89 (190.0)	-7.53 (-90.0)	6.00 (-213.8)	-8.80 (313.8)
4-B	-6.08 (106.7)	0.38 (-6.7)	-1.07 (105.5)	0.06 (-5.5)	-2.14 (109.8)	0.19 (-9.8)	-0.19 (28.3)	-0.49 (71.7)
5-B	0.33 (110.7)	-0.03 (-10.7)	0.07	0.03	0.28 (103.9)	-0.01 (-3.9)	0.06	0.05
6-B	0.11 (98.0)	0.002 (2.0)	-0.005	-0.003	-0.03	0.001	-0.004	0.001
7-B	-0.04	0.000	0.000	0.000	0.003	0.000	0.000	0.000
8-B	0.008	0.000	0.000	0.000	0.000	0.000	0.000	0.000
9-B	-0.001	0.000	0.000	0.000	0.000	0.000	0.000	0.000
10-B	0.000	0.000	0.000	0.000	0.000	0.000	0.000	0.000
Total	**-169.32 (94.7)**	**-9.46 (5.3)**	**-155.32 (89.1)**	**-19.06 (10.9)**	**-68.82 (77.3)**	**-20.21 (22.7)**	**-57.92 (60.9)**	**-37.18 (39.1)**

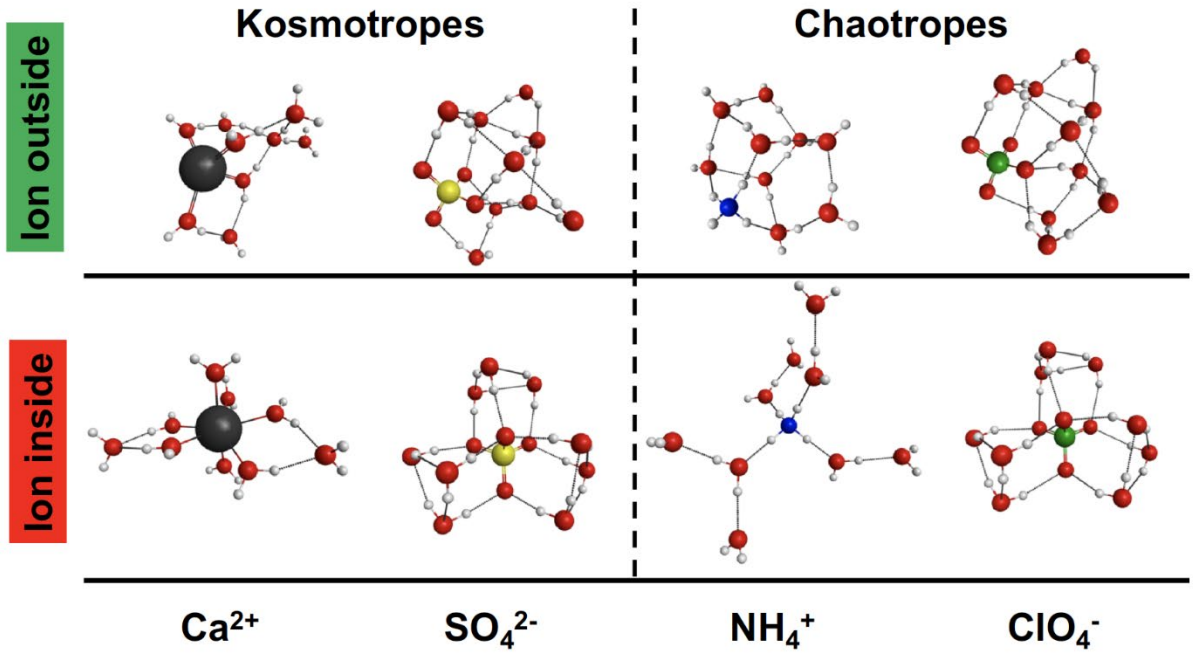

Figure 1. The geometries of the aqueous ionic clusters with the ion outside (top row) and inside (bottom row) a water cluster network. The Cartesian coordinates are included in the Supporting Information.

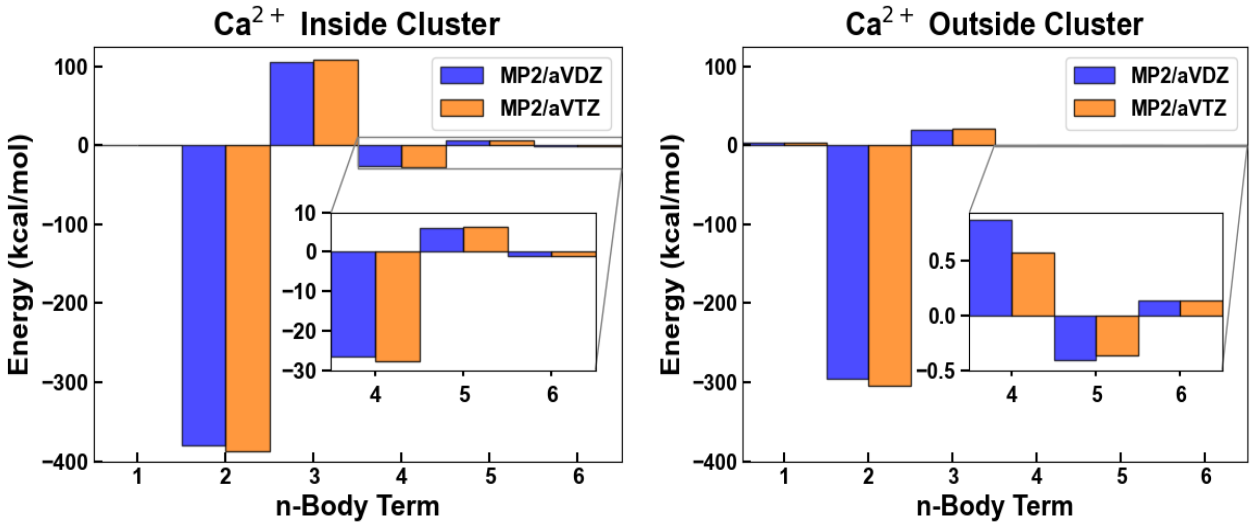

Figure 2. Relative magnitudes of the M-B terms up to 6-B for the two isomers of the $Ca^{2+}(H_2O)_9$ cluster at the MP2 level of theory including BSSE corrections with the aVDZ (blue) and aVTZ (orange) basis sets.

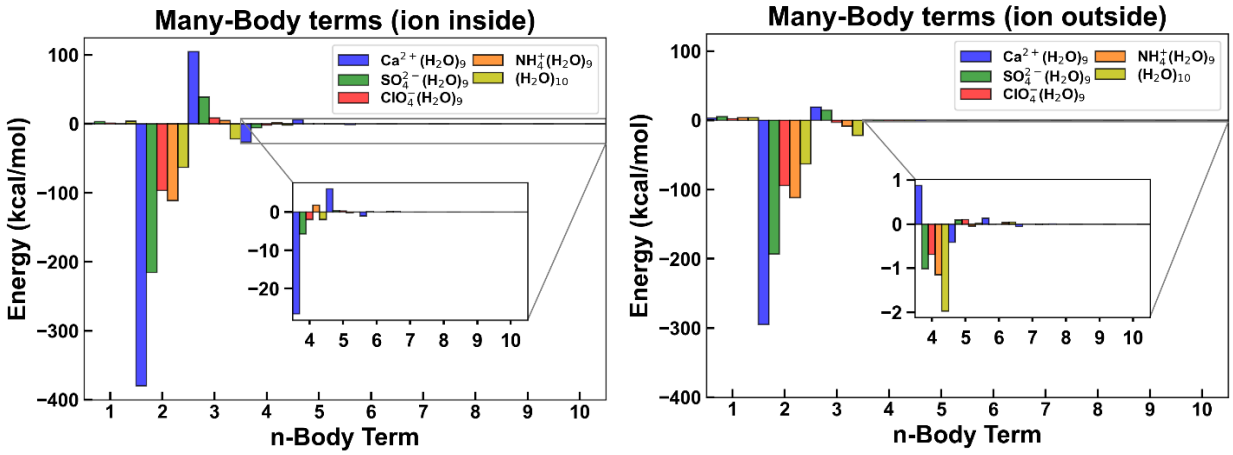

Figure 3. Many-body terms of each ion cluster $X^{+/-}(H_2O)_9$ and $(H_2O)_{10}$ for the ion inside (top panel) and ion outside (bottom panel) geometries.

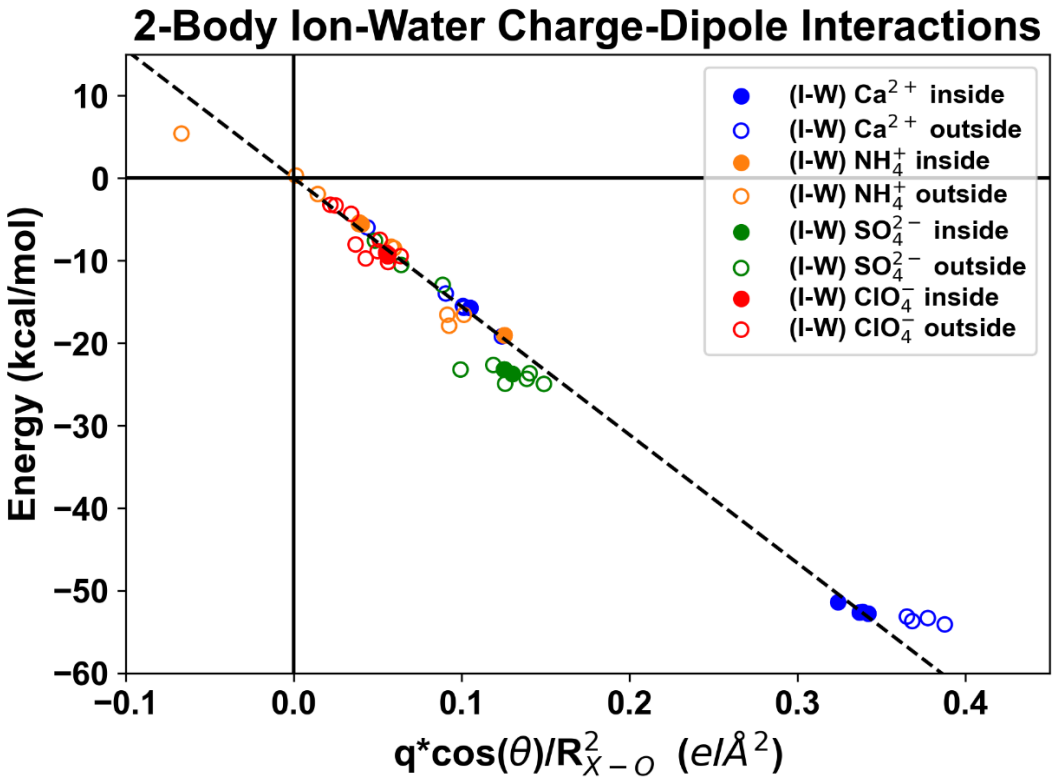

Figure 4. Individual 2-B (I-W) contributions to the total BSSE correction for the various ions as a function of $q \cdot \cos(\theta)/R_{X-O}^2$. The linear fit (broken line) has a slope of -155.60 (R^2 = 0.9777).

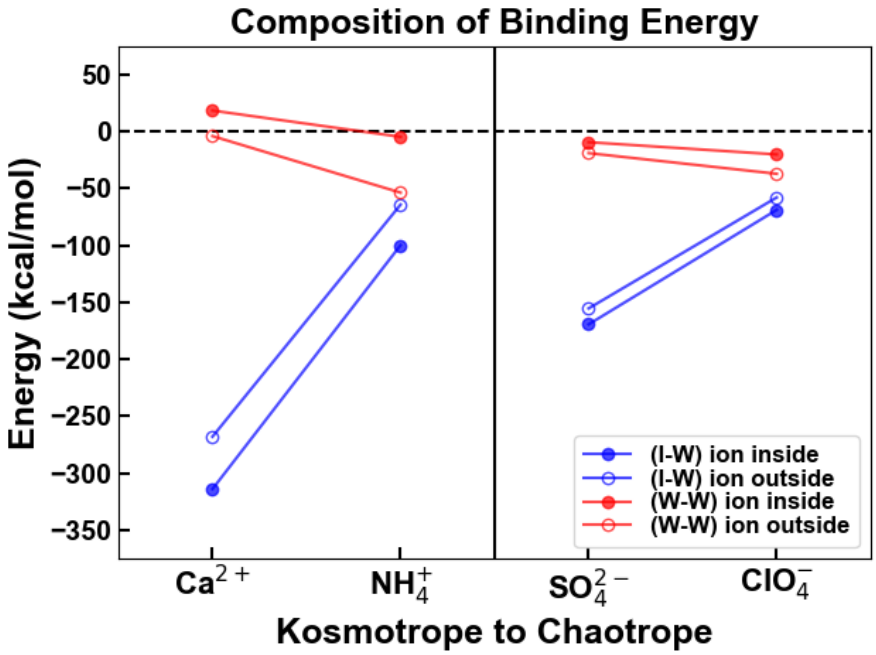

Figure 5. The composition of the total cluster binding energy in terms of the (I-W) and (W-W) interactions for the configurations with the ions residing on the outside (open circles) and the inside (filled circles) of the aqueous cluster. All numbers are corrected for BSSE.

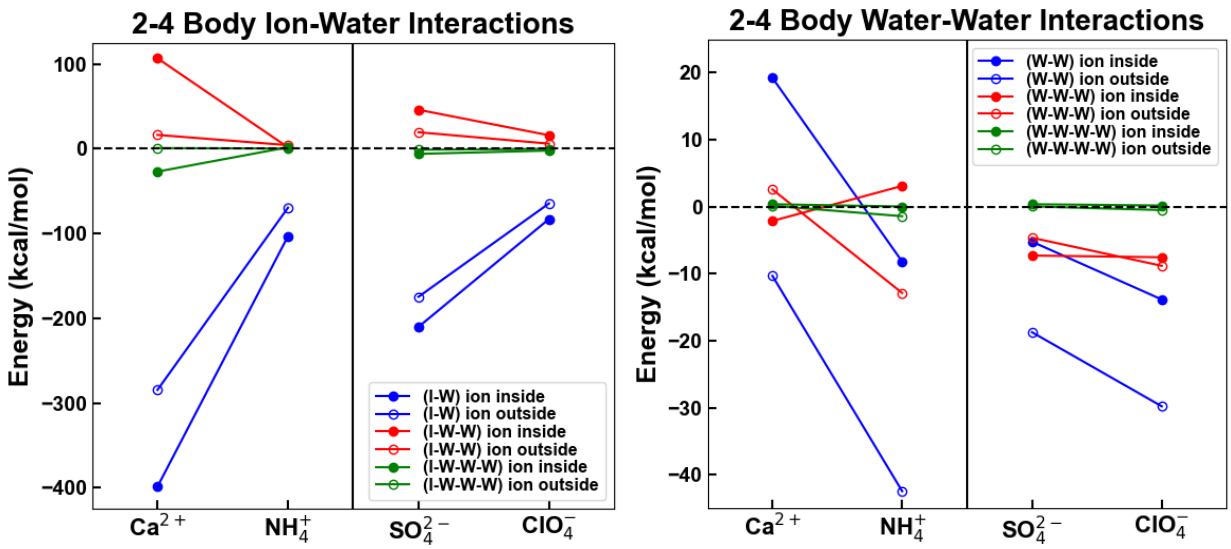

Figure 6. Ion-water (left panel) and water-water (right panel) contributions to the 2-, 3-, and 4-B terms of the Hofmeister ions considered in this study. The same plotting conventions with Figure 4 are used. All numbers are corrected for BSSE.

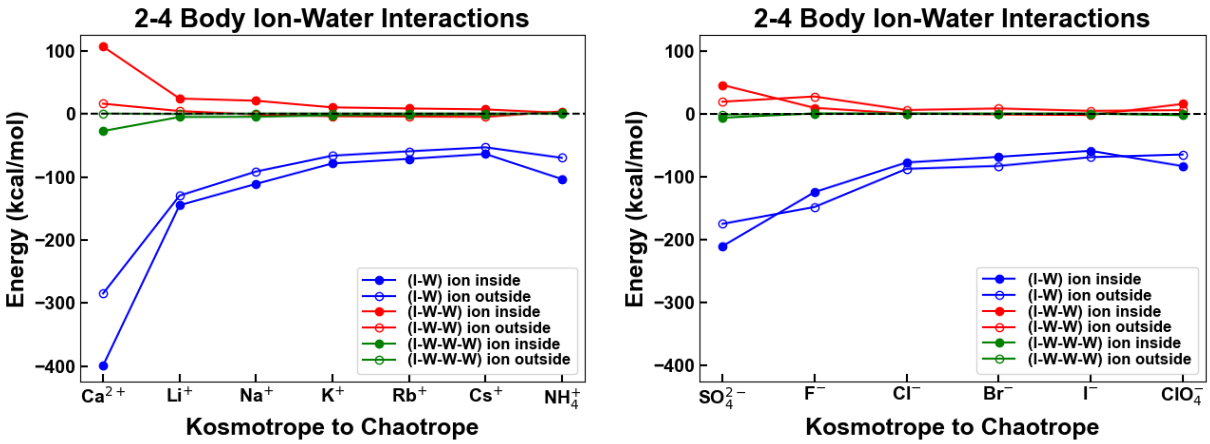

Figure 7. Ion-water contributions to the 2-B (blue), 3-B (red), and 4-B (green) terns of the MBE. Previously reported monatomic ions in the middle of the Hofmeister series are included.[46] The same plotting conventions with Figure 5 are used. All numbers are corrected for BSSE.

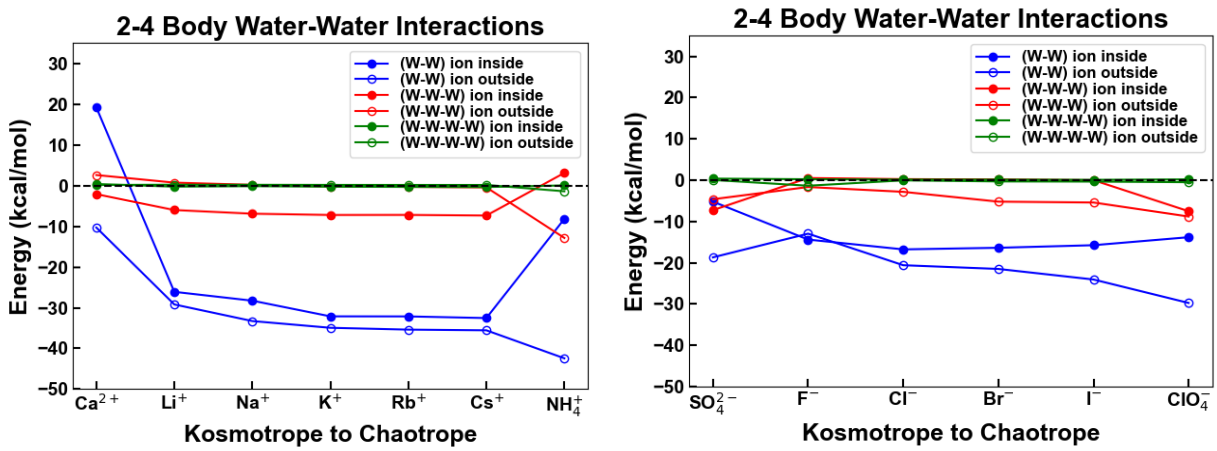

Figure 8. Water-water contributions to the 2-B (blue), 3-B (red), and 4-B (green) terms of the MBE. Previously reported monatomic ions in the middle of the Hofmeister series are included.[46] The same plotting conventions with Figure 5 are used. All numbers are corrected for BSSE.

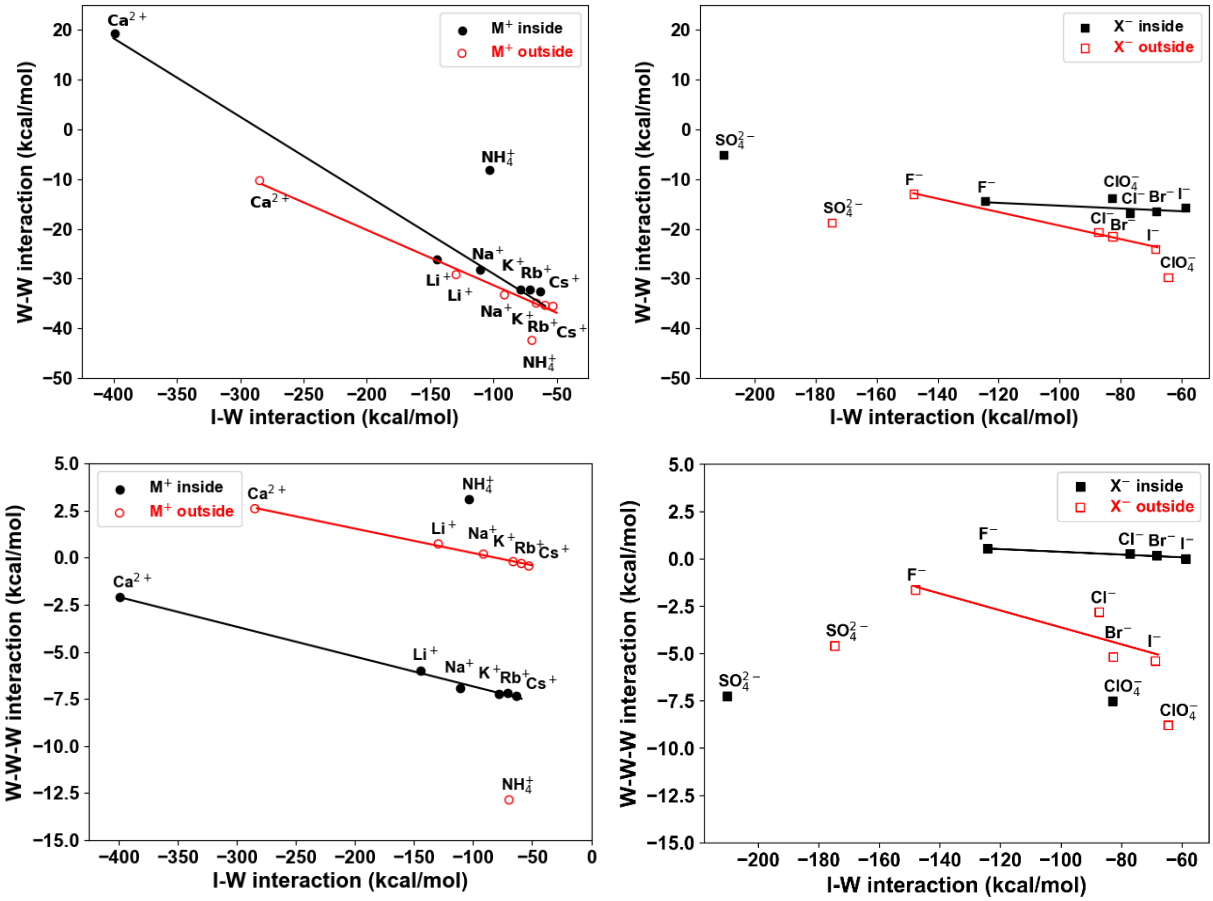

Figure 9. Correlations between various interactions for $Z^{+/-}(H_2O)_9$ where Z = Ca^{2+}, NH_4^+, Li^+, Na^+ K^+, Rb^+, Cs^+ (left panel) and Z = SO_4^{2-}, ClO_4^-, F^-, Cl^-, Br^-, I^- (right panel): (W-W) vs. (I-W) (top panels) and (W-W-W) vs. (I-W) (bottom panels).[46] Linear trends are shown for monatomic ions.

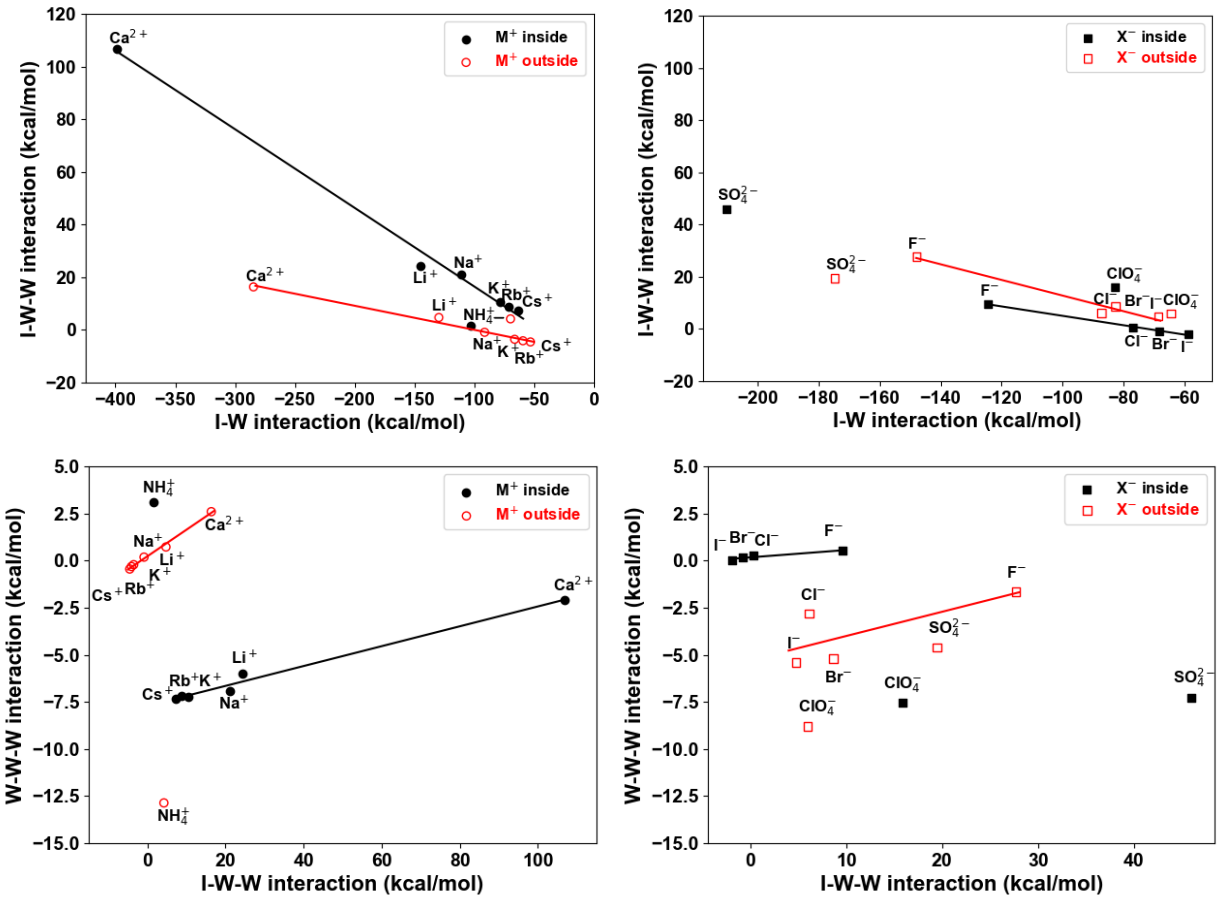

Figure 10. Correlations between various interactions for $Z^{+/-}(H_2O)_9$ where Z = Ca^{2+}, NH_4^+, Li^+, Na^+, K^+, Rb^+, Cs^+ (left panel) and Z = SO_4^{2-}, ClO_4^-, F^-, Cl^-, Br^-, I^- (right panel): (I-W-W) vs. (I-W) (top panels) and (W-W-W) vs. (I-W-W) (bottom panels).[46] Linear fits are shown for monatomic ions.

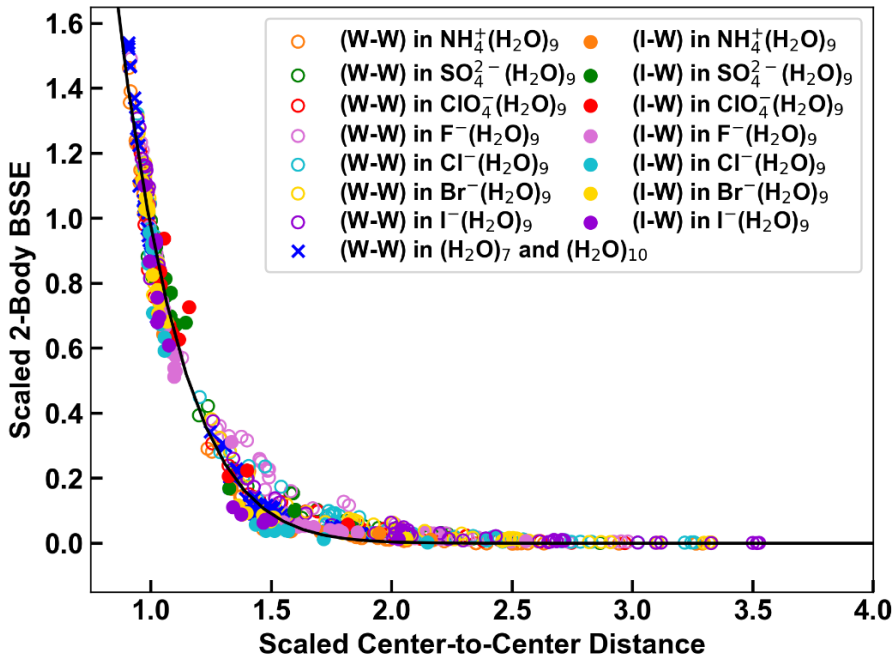

Figure 11. Scaled 2-B (W-W) and (I-W) BSSE corrections for $Z^{+/-}(H_2O)_9$ where Z = NH_4^+, SO_4^{2-}, ClO_4^-, Cl^-, Br^-, I^- and scaled 2-B (W-W) BSSE corrections for $(H_2O)_7$ and $(H_2O)_{10}$ fit to equation (8) (a = 14.11, b = 1.29, R^2 = 0.9840).[45,46]

REFERENCES

(1) Hofmeister, F. Zur Lehre von Der Wirkung Der Salze. *Arch. F Exp. Pathol U Pharmakol* **1888**, No. 25, 1–30. https://doi.org/10.1007/BF01838161.

(2) Kunz, W.; Henle, J.; Ninham, B. W. 'Zur Lehre von Der Wirkung Der Salze' (about the Science of the Effect of Salts): Franz Hofmeister's Historical Papers. *Curr. Opin. Colloid Interface Sci.* **2004**, *9* (1), 19–37. https://doi.org/10.1016/j.cocis.2004.05.005.

(3) Jones, G.; Dole, M. THE VISCOSITY OF AQUEOUS SOLUTIONS OF STRONG ELECTROLYTES WITH SPECIAL REFERENCE TO BARIUM CHLORIDE. *J. Am. Chem. Soc.* **1929**, *51* (10), 2950–2964. https://doi.org/10.1021/ja01385a012.

(4) Jenkins, H. D. B.; Marcus, Yizhak. Viscosity B-Coefficients of Ions in Solution. *Chem. Rev.* **1995**, *95* (8), 2695–2724. https://doi.org/10.1021/cr00040a004.

(5) Boström, M.; Kunz, W.; Ninham, B. W. Hofmeister Effects in Surface Tension of Aqueous Electrolyte Solution. *Langmuir* **2005**, *21* (6), 2619–2623. https://doi.org/10.1021/la047437v.

(6) Pegram, L. M.; Record, M. T. Hofmeister Salt Effects on Surface Tension Arise from Partitioning of Anions and Cations between Bulk Water and the Air−Water Interface. *J. Phys. Chem. B* **2007**, *111* (19), 5411–5417. https://doi.org/10.1021/jp070245z.

(7) Xie, W. J.; Gao, Y. Q. A Simple Theory for the Hofmeister Series. *J. Phys. Chem. Lett.* **2013**, *4* (24), 4247–4252. https://doi.org/10.1021/jz402072g.

(8) Willow, S. Y.; Xantheas, S. S. Molecular-Level Insight of the Effect of Hofmeister Anions on the Interfacial Surface Tension of a Model Protein. *J. Phys. Chem. Lett.* **2017**, *8* (7), 1574–1577. https://doi.org/10.1021/acs.jpclett.7b00069.

(9) Baldwin, R. L. How Hofmeister Ion Interactions Affect Protein Stability. *Biophys. J.* **1996**, *71* (4), 2056–2063. https://doi.org/10.1016/S0006-3495(96)79404-3.

(10) Okur, H. I.; Hladílková, J.; Rembert, K. B.; Cho, Y.; Heyda, J.; Dzubiella, J.; Cremer, P. S.; Jungwirth, P. Beyond the Hofmeister Series: Ion-Specific Effects on Proteins and Their Biological Functions. *J. Phys. Chem. B* **2017**, *121* (9), 1997–2014. https://doi.org/10.1021/acs.jpcb.6b10797.

(11) Shimizu, S.; McLaren, W. M.; Matubayasi, N. The Hofmeister Series and Protein-Salt Interactions. *J. Chem. Phys.* **2006**, *124* (23), 234905. https://doi.org/10.1063/1.2206174.

(12) Collins, K. D. Ions from the Hofmeister Series and Osmolytes: Effects on Proteins in Solution and in the Crystallization Process. *Methods* **2004**, *34* (3), 300–311. https://doi.org/10.1016/j.ymeth.2004.03.021.

(13) Perez-Jimenez, R.; Godoy-Ruiz, R.; Ibarra-Molero, B.; Sanchez-Ruiz, J. M. The Efficiency of Different Salts to Screen Charge Interactions in Proteins: A Hofmeister Effect? *Biophys. J.* **2004**, *86* (4), 2414–2429. https://doi.org/10.1016/S0006-3495(04)74298-8.

(14) Zhang, Y.; Cremer, P. Interactions between Macromolecules and Ions: The Hofmeister Series. *Curr. Opin. Chem. Biol.* **2006**, *10* (6), 658–663. https://doi.org/10.1016/j.cbpa.2006.09.020.

(15) Lund, M.; Jungwirth, P. Patchy Proteins, Anions and the Hofmeister Series. *J. Phys. Condens. Matter* **2008**, *20* (49), 494218. https://doi.org/10.1088/0953-8984/20/49/494218.

(16) Sedlák, E.; Stagg, L.; Wittung-Stafshede, P. Effect of Hofmeister Ions on Protein Thermal Stability: Roles of Ion Hydration and Peptide Groups? *Arch. Biochem. Biophys.* **2008**, *479* (1), 69–73. https://doi.org/10.1016/j.abb.2008.08.013.

(17) Piazza, R.; Pierno, M. Protein Interactions near Crystallization: A Microscopic Approach to the Hofmeister Series. *J. Phys. Condens. Matter* **2000**, *12* (8A), A443–A449. https://doi.org/10.1088/0953-8984/12/8A/361.
(18) Schneider, C. P.; Shukla, D.; Trout, B. L. Arginine and the Hofmeister Series: The Role of Ion–Ion Interactions in Protein Aggregation Suppression. *J. Phys. Chem. B* **2011**, *115* (22), 7447–7458. https://doi.org/10.1021/jp111920y.
(19) Boström, M.; Williams, D. R. M.; Ninham, B. W. Why the Properties of Proteins in Salt Solutions Follow a Hofmeister Series. *Curr. Opin. Colloid Interface Sci.* **2004**, *9* (1), 48–52. https://doi.org/10.1016/j.cocis.2004.05.001.
(20) Tadeo, X.; López-Méndez, B.; Castaño, D.; Trigueros, T.; Millet, O. Protein Stabilization and the Hofmeister Effect: The Role of Hydrophobic Solvation. *Biophys. J.* **2009**, *97* (9), 2595–2603. https://doi.org/10.1016/j.bpj.2009.08.029.
(21) Fox, J. M.; Kang, K.; Sherman, W.; Héroux, A.; Sastry, G. M.; Baghbanzadeh, M.; Lockett, M. R.; Whitesides, G. M. Interactions between Hofmeister Anions and the Binding Pocket of a Protein. *J. Am. Chem. Soc.* **2015**, *137* (11), 3859–3866. https://doi.org/10.1021/jacs.5b00187.
(22) Moreira, L. A.; Boström, M.; Ninham, B. W.; Biscaia, E. C.; Tavares, F. W. Hofmeister Effects: Why Protein Charge, PH Titration and Protein Precipitation Depend on the Choice of Background Salt Solution. *Colloids Surf. Physicochem. Eng. Asp.* **2006**, *282–283*, 457–463. https://doi.org/10.1016/j.colsurfa.2005.11.021.
(23) Chen, Y.; Okur, H. I.; Gomopoulos, N.; Macias-Romero, C.; Cremer, P. S.; Petersen, P. B.; Tocci, G.; Wilkins, D. M.; Liang, C.; Ceriotti, M.; Roke, S. Electrolytes Induce Long-Range Orientational Order and Free Energy Changes in the H-Bond Network of Bulk Water. *Sci. Adv.* **2016**, *2* (4), e1501891. https://doi.org/10.1126/sciadv.1501891.
(24) Shalit, A.; Ahmed, S.; Savolainen, J.; Hamm, P. Terahertz Echoes Reveal the Inhomogeneity of Aqueous Salt Solutions. *Nat. Chem.* **2017**, *9* (3), 273–278. https://doi.org/10.1038/nchem.2642.
(25) Petersen, P. B.; Saykally, R. J. On the Nature of Ions at the Liquid Water Surface. *Annu. Rev. Phys. Chem.* **2006**, *57* (1), 333–364. https://doi.org/10.1146/annurev.physchem.57.032905.104609.
(26) Cappa, C. D.; Smith, J. D.; Messer, B. M.; Cohen, R. C.; Saykally, R. J. Effects of Cations on the Hydrogen Bond Network of Liquid Water: New Results from X-Ray Absorption Spectroscopy of Liquid Microjets. *J. Phys. Chem. B* **2006**, *110* (11), 5301–5309. https://doi.org/10.1021/jp054699c.
(27) Pollard, T. P.; Beck, T. L. Toward a Quantitative Theory of Hofmeister Phenomena: From Quantum Effects to Thermodynamics. *Curr. Opin. Colloid Interface Sci.* **2016**, *23*, 110–118. https://doi.org/10.1016/j.cocis.2016.06.015.
(28) O'Brien, J. T.; Williams, E. R. Effects of Ions on Hydrogen-Bonding Water Networks in Large Aqueous Nanodrops. *J. Am. Chem. Soc.* **2012**, *134* (24), 10228–10236. https://doi.org/10.1021/ja303191r.
(29) O'Brien, J. T.; Prell, J. S.; Bush, M. F.; Williams, E. R. Sulfate Ion Patterns Water at Long Distance. *J. Am. Chem. Soc.* **2010**, *132* (24), 8248–8249. https://doi.org/10.1021/ja1024113.
(30) DiTucci, M. J.; Heiles, S.; Williams, E. R. Role of Water in Stabilizing Ferricyanide Trianion and Ion-Induced Effects to the Hydrogen-Bonding Water Network at Long

Distance. *J. Am. Chem. Soc.* **2015**, *137* (4), 1650–1657. https://doi.org/10.1021/ja5119545.
(31) Yan, C.; Xue, Z.; Zhao, W.; Wang, J.; Mu, T. Surprising Hofmeister Effects on the Bending Vibration of Water. *ChemPhysChem* **2016**, *17* (20), 3309–3314. https://doi.org/10.1002/cphc.201600551.
(32) Mancinelli, R.; Botti, A.; Bruni, F.; Ricci, M. A.; Soper, A. K. Hydration of Sodium, Potassium, and Chloride Ions in Solution and the Concept of Structure Maker/Breaker. *J. Phys. Chem. B* **2007**, *111* (48), 13570–13577. https://doi.org/10.1021/jp075913v.
(33) Omta, A. W. Negligible Effect of Ions on the Hydrogen-Bond Structure in Liquid Water. *Science* **2003**, *301* (5631), 347–349. https://doi.org/10.1126/science.1084801.
(34) Wachter, W.; Kunz, W.; Buchner, R.; Hefter, G. Is There an Anionic Hofmeister Effect on Water Dynamics? Dielectric Spectroscopy of Aqueous Solutions of NaBr, NaI, $NaNO_3$, $NaClO_4$, and NaSCN. *J. Phys. Chem. A* **2005**, *109* (39), 8675–8683. https://doi.org/10.1021/jp053299m.
(35) Näslund, L.-Å.; Edwards, D. C.; Wernet, P.; Bergmann, U.; Ogasawara, H.; Pettersson, L. G. M.; Myneni, S.; Nilsson, A. X-Ray Absorption Spectroscopy Study of the Hydrogen Bond Network in the Bulk Water of Aqueous Solutions. *J. Phys. Chem. A* **2005**, *109* (27), 5995–6002. https://doi.org/10.1021/jp050413s.
(36) Yin, Z.; Rajkovic, I.; Kubicek, K.; Quevedo, W.; Pietzsch, A.; Wernet, P.; Föhlisch, A.; Techert, S. Probing the Hofmeister Effect with Ultrafast Core–Hole Spectroscopy. *J. Phys. Chem. B* **2014**, *118* (31), 9398–9403. https://doi.org/10.1021/jp504577a.
(37) Jungwirth, P.; Tobias, D. J. Ions at the Air/Water Interface. *J. Phys. Chem. B* **2002**, *106* (25), 6361–6373. https://doi.org/10.1021/jp020242g.
(38) Galamba, N. Mapping Structural Perturbations of Water in Ionic Solutions. *J. Phys. Chem. B* **2012**, *116* (17), 5242–5250. https://doi.org/10.1021/jp3014578.
(39) Mountain, R. D. Alterations in Water Structure Induced by Guanidinium and Sodium Ions. 6.
(40) Gaiduk, A. P.; Galli, G. Local and Global Effects of Dissolved Sodium Chloride on the Structure of Water. *J. Phys. Chem. Lett.* **2017**, *8* (7), 1496–1502. https://doi.org/10.1021/acs.jpclett.7b00239.
(41) Grossfield, A. Dependence of Ion Hydration on the Sign of the Ion's Charge. *J. Chem. Phys.* **2005**, *122* (2), 024506. https://doi.org/10.1063/1.1829036.
(42) Baer, M. D.; Mundy, C. J. An Ab Initio Approach to Understanding the Specific Ion Effect. *Faraday Discuss* **2013**, *160*, 89–101. https://doi.org/10.1039/C2FD20113E.
(43) Schwenk, C. F.; Hofer, T. S.; Rode, B. M. "Structure Breaking" Effect of Hydrated Cs^+. *J. Phys. Chem. A* **2004**, *108* (9), 1509–1514. https://doi.org/10.1021/jp037179v.
(44) Leberman, R.; Soper, A. K. Effect of High Salt Concentrations on Water Structure. *Nature* **1995**, *378* (6555), 364–366. https://doi.org/10.1038/378364a0.
(45) Heindel, J. P.; Xantheas, S. S. The Many-Body Expansion for Aqueous Systems Revisited: I. Water–Water Interactions. *J. Chem. Theory Comput.* **2020**, *16* (11), 6843–6855. https://doi.org/10.1021/acs.jctc.9b00749.
(46) Heindel, J.; Xantheas, S. The Many-Body Expansion for Aqueous Systems Revisited: II. Alkali Metal and Halide Ion-Water Interactions. *J. Chem. Theory Comput.* in press (2020). https://dx.doi.org/10.1021/acs.jctc.0c01309.
(47) Roberts, F.; Tesman, B. U. *Applied Combinatorics, Second Edition*; Taylor & Francis, 2009.

(48) Hankins, D.; Moskowitz, J. W.; Stillinger, F. H. Water Molecule Interactions. *J. Chem. Phys.* **1970**, *53* (12), 4544–4554. https://doi.org/10.1063/1.1673986.
(49) Xantheas, S. S. *Ab Initio* Studies of Cyclic Water Clusters $(H_2O)_n$, n =1–6. II. Analysis of Many-body Interactions. *J. Chem. Phys.* **1994**, *100* (10), 7523–7534. https://doi.org/10.1063/1.466846.
(50) Xantheas, S. S. On the Importance of the Fragment Relaxation Energy Terms in the Estimation of the Basis Set Superposition Error Correction to the Intermolecular Interaction Energy. *J. Chem. Phys.* **1996**, *104* (21), 8821–8824. https://doi.org/10.1063/1.471605.
(51) White, J. C.; Davidson, E. R. An Analysis of the Hydrogen Bond in Ice. *J. Chem. Phys.* **1990**, *93* (11), 8029–8035. https://doi.org/10.1063/1.459332.
(52) Xantheas, S. S. Significance of Higher-Order Many-Body Interaction Energy Terms in Water Clusters and Bulk Water. *Philos. Mag. B* **2006**. https://doi.org/10.1080/13642819608239116.
(53) Xantheas, S. S. Cooperativity and Hydrogen Bonding Network in Water Clusters. *Chem. Phys.* **2000**, *258* (2–3), 225–231. https://doi.org/10.1016/S0301-0104(00)00189-0.
(54) Marcus, Y.; Hefter, G. Ion Pairing. *Chem. Rev.* **2006**, *106* (11), 4585–4621. https://doi.org/10.1021/cr040087x.
(55) Fennell, C. J.; Bizjak, A.; Vlachy, V.; Dill, K. A. Ion Pairing in Molecular Simulations of Aqueous Alkali Halide Solutions. *J. Phys. Chem. B* **2009**, *113* (19), 6782–6791. https://doi.org/10.1021/jp809782z.
(56) Götte, L.; Parry, K. M.; Hua, W.; Verreault, D.; Allen, H. C.; Tobias, D. J. Solvent-Shared Ion Pairs at the Air–Solution Interface of Magnesium Chloride and Sulfate Solutions Revealed by Sum Frequency Spectroscopy and Molecular Dynamics Simulations. *J. Phys. Chem. A* **2017**, *121* (34), 6450–6459. https://doi.org/10.1021/acs.jpca.7b05600.
(57) González, B. S.; Hernández-Rojas, J.; Wales, D. J. Global Minima and Energetics of Li+(H2O)n and Ca2+(H2O)n Clusters for N⩽20. *Chem. Phys. Lett.* **2005**, *412* (1), 23–28. https://doi.org/10.1016/j.cplett.2005.06.090.
(58) Pei, S.-T.; Jiang, S.; Liu, Y.-R.; Huang, T.; Xu, K.-M.; Wen, H.; Zhu, Y.-P.; Huang, W. Properties of Ammonium Ion–Water Clusters: Analyses of Structure Evolution, Noncovalent Interactions, and Temperature and Humidity Effects. *J. Phys. Chem. A* **2015**, *119* (12), 3035–3047. https://doi.org/10.1021/jp512323k.
(59) Kulichenko, M.; Fedik, N.; Bozhenko, K. V.; Boldyrev, A. I. Hydrated Sulfate Clusters $SO_4^{2-}(H_2O)_n$ (n = 1–40): Charge Distribution Through Solvation Shells and Stabilization. *J. Phys. Chem. B* **2019**, *123* (18), 4065–4069. https://doi.org/10.1021/acs.jpcb.9b01744.
(60) Lambrecht, D. S.; Clark, G. N. I.; Head-Gordon, T.; Head-Gordon, M. Exploring the Rich Energy Landscape of Sulfate–Water Clusters $SO_4^{2-}(H_2O)_{n=3-7}$: An Electronic Structure Approach. *J. Phys. Chem. A* **2011**, *115* (41), 11438–11454. https://doi.org/10.1021/jp206064n.
(61) Dunning, T. H. Gaussian Basis Sets for Use in Correlated Molecular Calculations. I. The Atoms Boron through Neon and Hydrogen. *J. Chem. Phys.* **1989**, *90* (2), 1007–1023. https://doi.org/10.1063/1.456153.
(62) Kaupp, M.; Schleyer, P. v. R.; Stoll, H.; Preuss, H. Pseudopotential Approaches to Ca, Sr, and Ba Hydrides. Why Are Some Alkaline Earth MX_2 Compounds Bent? *J. Chem. Phys.* **1991**, *94* (2), 1360–1366. https://doi.org/10.1063/1.459993.

(63) Boys, S. F.; Bernardi, F. The Calculation of Small Molecular Interactions by the Differences of Separate Total Energies. Some Procedures with Reduced Errors. *Mol. Phys.* **1970**, *19* (4), 553–566. https://doi.org/10.1080/00268977000101561.
(64) Valiev, M.; Bylaska, E. J.; Govind, N.; Kowalski, K.; Straatsma, T. P.; Van Dam, H. J. J.; Wang, D.; Nieplocha, J.; Apra, E.; Windus, T. L.; de Jong, W. A. NWChem: A Comprehensive and Scalable Open-Source Solution for Large Scale Molecular Simulations. *Comput. Phys. Commun.* **2010**, *181* (9), 1477–1489. https://doi.org/10.1016/j.cpc.2010.04.018.
(65) Collins, K. D. Charge Density-Dependent Strength of Hydration and Biological Structure. *Biophys. J.* **1997**, *72* (1), 65–76. https://doi.org/10.1016/S0006-3495(97)78647-8.
(66) Guo, F.; Friedman, J. M. Charge Density-Dependent Modifications of Hydration Shell Waters by Hofmeister Ions. *J. Am. Chem. Soc.* **2009**, *131* (31), 11010–11018. https://doi.org/10.1021/ja902240j.
(67) Collins, K. D. Sticky Ions in Biological Systems. *Proc. Natl. Acad. Sci.* **1995**, *92* (12), 5553–5557. https://doi.org/10.1073/pnas.92.12.5553.
(68) Parsons, D. F.; Boström, M.; Nostro, P. L.; Ninham, B. W. Hofmeister Effects: Interplay of Hydration, Nonelectrostatic Potentials, and Ion Size. *Phys. Chem. Chem. Phys.* **2011**, *13* (27), 12352. https://doi.org/10.1039/c1cp20538b.
(69) Hribar, B.; Southall, N. T.; Vlachy, V.; Dill, K. A. How Ions Affect the Structure of Water. *J. Am. Chem. Soc.* **2002**, *124* (41), 12302–12311. https://doi.org/10.1021/ja026014h.
(70) Werhahn, J. C.; Akase, D.; Xantheas, S. S. Universal Scaling of Potential Energy Functions Describing Intermolecular Interactions. II. The Halide-Water and Alkali Metal-Water Interactions. *J. Chem. Phys.* **2014**, *141* (6), 064118. https://doi.org/10.1063/1.4891820.
(71) Werhahn, J. C.; Miliordos, E.; Xantheas, S. S. A New Variation of the Buckingham Exponential-6 Potential with a Tunable, Singularity-Free Short-Range Repulsion and an Adjustable Long-Range Attraction. *Chem. Phys. Lett.* **2015**, *619*, 133–138. https://doi.org/10.1016/j.cplett.2014.11.051.
(72) Xantheas, S. S.; Werhahn, J. C. Universal Scaling of Potential Energy Functions Describing Intermolecular Interactions. I. Foundations and Scalable Forms of New Generalized Mie, Lennard-Jones, Morse, and Buckingham Exponential-6 Potentials. *J. Chem. Phys.* **2014**, *141* (6), 064117. https://doi.org/10.1063/1.4891819.
(73) Sharma, B.; Chandra, A. Ab Initio Molecular Dynamics Simulation of the Phosphate Ion in Water: Insights into Solvation Shell Structure, Dynamics, and Kosmotropic Activity. *J. Phys. Chem. B* **2017**, *121* (46), 10519–10529. https://doi.org/10.1021/acs.jpcb.7b06091.
(74) Bakker, H. J.; Kropman, M. F.; Omta, A. W.; Woutersen, S. Hydrogen-Bond Dynamics of Water in Ionic Solutions. *Phys. Scr.* **2004**, *69* (6), C14. https://doi.org/10.1238/Physica.Regular.069a00C14.
(75) Arismendi-Arrieta, D. J.; Riera, M.; Bajaj, P.; Prosmiti, R.; Paesani, F., I-TTM model for ab initio-based ion–water interaction potentials. 1. Halide–water potential energy functions. *J. Phys. Chem. B* **2015,** *120*, 1822-1832.
(76) Riera, M.; Götz, A. W.; Paesani, F., The i-TTM model for ab initio-based ion–water interaction potentials. II. Alkali metal ion–water potential energy functions. *Physical Chemistry Chemical Physics* **2016,** *18*, 30334-30343.

(77) Babin, V.; Medders, G. R.; Paesani, F., Toward a Universal Water Model: First Principles Simulations from the Dimer to the Liquid Phase. *The Journal of Physical Chemistry Letters* **2012,** *3*, 3765-3769.